

## Electron-impact ionization of atomic hydrogen at incident electron energies of 15.6, 17.6, 25, and 40 eV

J. G. Childers,<sup>1</sup> K. E. James,<sup>1</sup> M. Hughes,<sup>1,\*</sup> Igor Bray,<sup>2</sup> M. Baertschy,<sup>3</sup> and M. A. Khakoo<sup>1</sup>

<sup>1</sup>Department of Physics, California State University, Fullerton, California 92834, USA

<sup>2</sup>Center for Atomic, Molecular and Surface Physics, School of Mathematical and Physical Sciences, Murdoch University, Perth 6150, Australia

<sup>3</sup>Department of Physics, University of Colorado, Denver, Colorado 80217, USA

(Received 19 February 2003; published 26 September 2003)

Absolute doubly differential cross sections for the electron-impact ionization of atomic hydrogen have been measured from near threshold to intermediate energies. The measurements are calibrated to the well-established, accurate differential cross section for electron-impact excitation of the atomic hydrogen transition  $H(1^2S \rightarrow 2^2S + 2^2P)$ . In these experiments background secondary electrons are suppressed by moving the atomic hydrogen target source to and from the collision region. Measurements cover the incident electron energy range of 14.6–40 eV, for scattering angles of  $10^\circ$ – $120^\circ$  and are found to be in very good agreement with the results of the most advanced theoretical models—the convergent close-coupling model and the exterior complex scaling model.

DOI: 10.1103/PhysRevA.68.030702

PACS number(s): 34.80.Dp

The electron-impact ionization of atomic hydrogen challenges theory by presenting it with the simplest three-body Coulomb system with two outgoing electrons in the vicinity of a proton. It is therefore the most transparent test, and the most significant at present, of the simplest many-body fermion problem. However, experimental differential cross sections for the electron-impact ionization of atomic hydrogen are sparse. The only available results are the absolute doubly differential cross section (DDCS) measurements of Shyn [1] and the triply differential cross sections (TDCS's) of Röder *et al.* [2]. *Ab initio*, theoretical models for the ionization of atomic hydrogen are the convergent close-coupling (CCC) model [3,4] and the more recent exterior complex scaling (ECS) model of Rescigno *et al.* [5]. Detailed comparison of ECS and CCC has been given by Baertschy *et al.* [6] with disagreement between the theories being largest at energies near the ionization threshold. Agreement of ECS with the relative TDCS measurements of Röder *et al.* [7] is superior to that of CCC. However, questions concerning the available absolute measurements of the TDCS [8,9] have prevented a definitive comparison between theory and experiment. Agreement between theory and the DDCS of Shyn [1] is satisfactory only at the lowest measured energy of 25 eV. At higher energies there is severe disagreement at both small and large scattering angles [10]. Thus, there has remained the need for reliable, absolute, differential measurements of  $e$ -H ionization.

In the present work, absolute DDCS's for the ionization of atomic hydrogen at low incident electron energies ( $E_0$ ) of 14.6, 15.6, 17.6, 20, 25, and 40 eV are measured. In this Rapid Communication, we present our 15.6-, 17.6-, 25-, and 40-eV measurements. Our apparatus has been discussed pre-

viously (see Ref. [11] and the references therein). The atomic beam is generated by an outside-silvered, sooted glass capillary needle and is made to cross a monochromatic beam of electrons from the electron gun of an electrostatic electron spectrometer in a conventional beam-beam configuration. Scattered electrons are detected by an electrostatic analyzer as a function of energy loss  $E_L$  and scattering angle  $\theta$ . The spectrometer performs with a typical incident electron current of  $\sim 60$ – $95$  nA with an energy resolution of about 120–150 meV (full width at half maximum, FWHM). This spectrometer has been proven to be stable over long periods ( $\sim 1$  y). The unit is baked at  $\sim 140^\circ\text{C}$  to maintain stability against oil contamination. The spectrometer is enclosed in a double mu-metal shield which reduces the magnetic field inside to less than 5 mG. The electron analyzer has an additional pupil placed at the focal point of a two-element lens before the entrance to the hemispherical analyzer. This restricts the depth-of-field of the instrument so that it observes electrons only from a small (5–6 mm) region of the collision

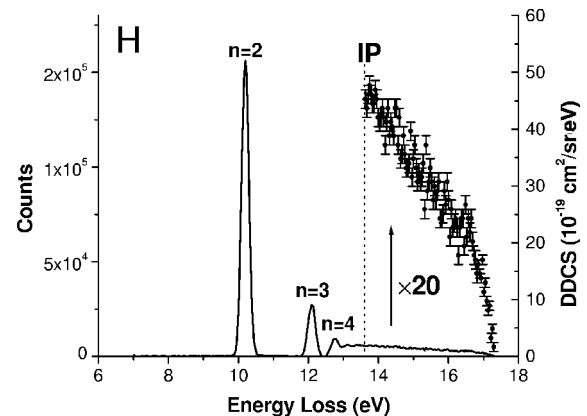


FIG. 1. Typical H spectrum resulting from all subtractions (i)–(iii) described in the text. IP labels the ionization potential. The continuum has been magnified by a factor of 20 and normalized.

\*Present address: Department of Physics, Magnolia High School, Anaheim, CA 92821.

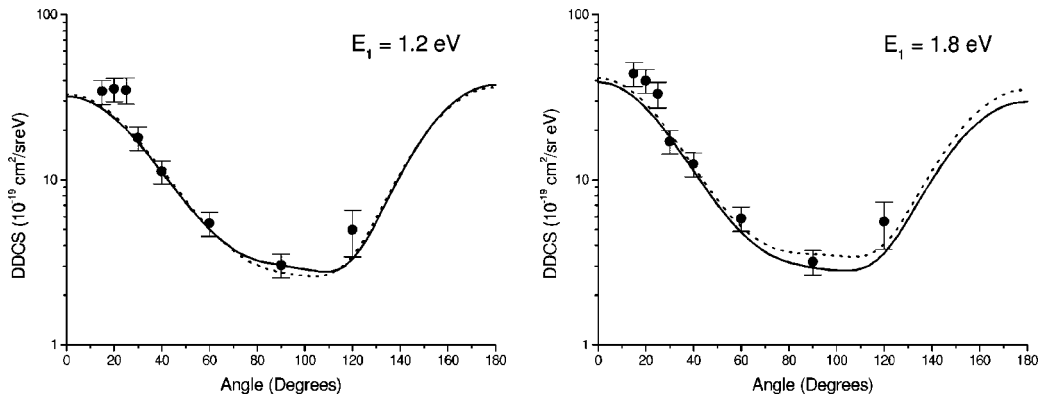


FIG. 2. Doubly differential cross sections for the electron-impact ionization of H at  $E_0 = 15.6$  eV obtained from the present experiments (●) and compared to the ECS [9] (—) and the recent CCC [15] (---) shown for different  $E_1$  values.

volume close to the capillary needle. The analyzer has a four-element zoom lens enabling it to transmit electrons from a wide range of kinetic energies with essentially constant efficiency. To determine the efficiency of the analyzer, we measured the spectrum of He at 31.7-eV incident electron energy and scattering angle of  $90^\circ$ . At this energy, the He ionization DDCS should be flat (within 10%) according to the Wannier law and as observed by, e.g., Keenan *et al.* [12]. Deviations from this are used to calibrate the analyzer's transmission response. To reduce the source of secondary electrons from surfaces in the experiment, the collision region is left open and all surfaces around the collision region, including the analyzer nose cone and aperture assembly, are liberally coated with soot from an acetylene flame. To further reduce secondary electrons, the incident electron beam is collimated by two exit apertures to produce a beam of pencil angle (FWHM) of about  $3^\circ$  and diameter less than 1.5 mm. Furthermore, the output electron gun optics has been modified so that the filling factor of the electron beam is at minimum approximately 0.5.

Our gas source—a recently developed, intense, and very stable H source—is detailed in Ref. [13]. It is an extended cavity microwave discharge of 99.999% purity  $H_2$  operating at 2450 MHz, and uses Teflon tubing to conduct the atoms to the outside-silvered glass needle. This source delivers H with a dissociation fraction of approximately 82–85% that is stable over periods exceeding a month.

Our measurements comprise electron-energy-loss spectra covering the  $E_L$  range of 6.5 eV to  $E_0 + 1$  eV. This covers the molecular hydrogen  $b^3\Sigma_u^+$  continuum and the full range of excited states including the ionization continuum of  $H_2$  which starts at 15.94 eV [14]. This range also covers the entire energy-loss spectrum of atomic hydrogen. To determine the background contribution to the scattered electron signal, we initially tried the conventional “chopper” design where a modulating flag is placed between the target gas beam and the collision region. This generated a secondary source of scattered electrons, especially in the low-kinetic-energy region, indistinguishable from the continuum. This method was therefore rejected. Instead, we rotate the graphite-coated capillary needle to and from the collision region using a compact “Hobby-Shack” vacuum-compatible servo-motor assembly mounted to the needle. Using this method, excellent background determination free from additional secondary electrons is observed for energies up to threshold. This has been verified by measuring identical background spectra with no gas in place with the needle in the IN (pointing toward the electron beam) and OUT (pointing at an angle of  $30^\circ$ – $40^\circ$  away) positions. Therefore the presence of the needle does not contribute additional secondary electrons. To prevent any possible deflection of the electron beam by the small magnetic field of the servo motor, the motor current is switched off once the needle is in place.

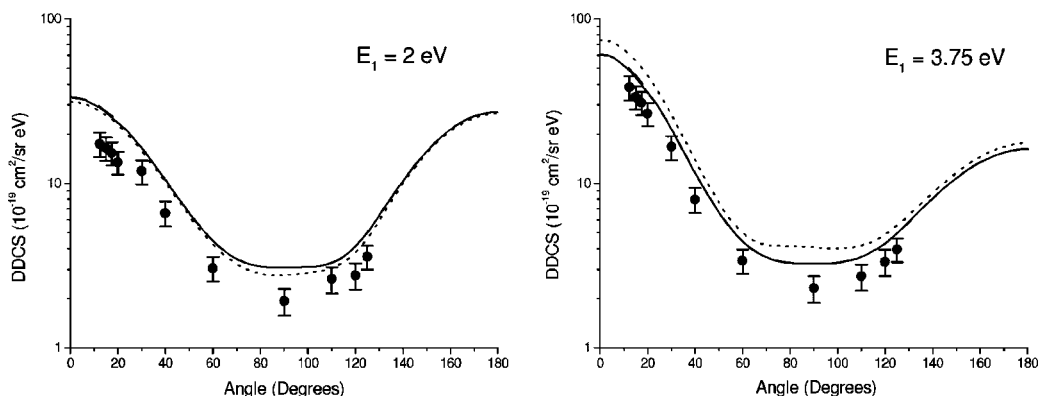


FIG. 3. Same as Fig. 2, but for  $E_0 = 17.6$  eV.

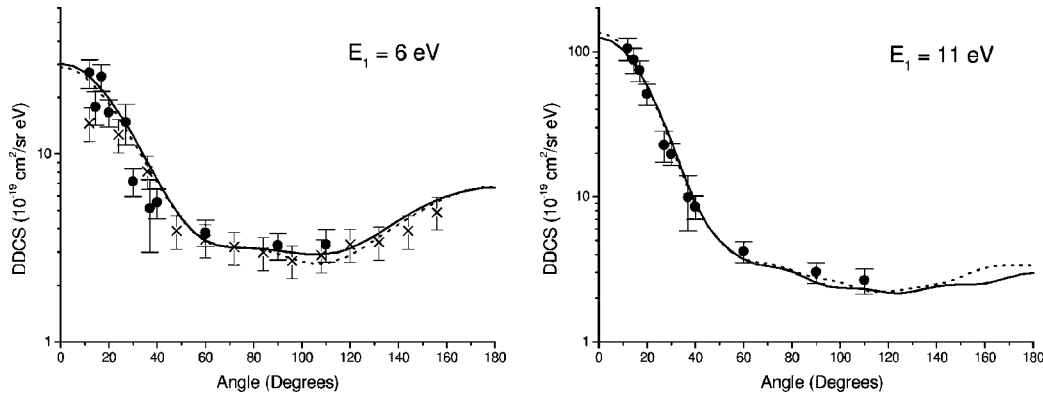


FIG. 4. Same as Fig. 2, but for  $E_0=25$  eV. The measurements of Shyn [1] ( $\times$ ) are also shown.

The electron-energy-loss spectra were measured with the discharge on and the gas cycling between the IN and OUT positions every 3 min until good statistics ( $<1\%$  typically) were acquired. This was repeated with the discharge off and the gas cycling between the IN and OUT positions every 3 min. The analysis of the spectra was performed as follows.

(i) The discharge on spectrum with gas beam OUT was subtracted from its corresponding discharge on spectrum with gas beam IN. This resulted in an electron-energy-loss spectrum of a  $H+H_2$  mixture with only gas-related scattering.

(ii) The discharge off spectrum with gas beam OUT was subtracted from the corresponding discharge off spectrum with gas beam IN. This resulted in an electron-energy-loss spectrum of  $H_2$  with only gas-related scattering.

(iii) The resultant  $H_2$  spectrum in (ii) was subtracted from the  $H+H_2$  spectrum in (i) after applying a scaling factor and allowing for small adjustments ( $<60$  meV) for drifts along the energy-loss scale. This scaled subtraction was critically determined (within 6% on average) by viewing the resultant spectrum and ensuring that there is no residual background in the energy-loss region between the  $H(n=2)$ ,  $H(n=3)$ , and  $H(n=4)$  energy-loss features (see Fig. 1).

The resultant pure spectrum of H, consisting of discrete states resolved up to  $n=3$ , partially resolved  $H(n=4)$ , and the continuum, was corrected for the transmission of the analyzer using the data from our He spectra [12] and cross sections from the CCC [16]. The transmission was found to be

reproducible within  $<15\%$ . A resultant H spectrum is shown in Fig. 1. This H spectrum (taken at  $E_0=17.6$  eV and  $\theta=20^\circ$ ) was normalized using the  $H(n=2)$  DCS obtained from the CCC [4], which have been tested experimentally [11,17] to be accurate on the sub-10% level. By fitting the continuum to a polynomial in energy loss of order  $\leq 2$ , we obtained the continuum doubly differential cross sections,

$$\frac{d^2\sigma(E_0, E_1, \theta)}{d\Omega dE} = \frac{N(E_1(\text{continuum}))}{N(n)} \frac{1}{\Delta E} \times \frac{\bar{T}(E_1(n=2))}{T(E_1(\text{continuum}))} \frac{d\sigma(n, E_0, \theta)}{d\Omega}, \quad (1)$$

where  $E_1=E_0-E_L$  is the residual electron energy,  $N(E_1(\text{continuum}))$  is the height of the continuum (number of electron scattering events) at the position  $E_1$  in the continuum,  $\Delta E$  is the step width per channel,  $N(n)$  is the intensity (number of electron scattering events) under the  $H(n; n=2, 3, \text{ or } 4)$  energy-loss line, and  $d\sigma(n, E_0, \theta)/d\Omega$  is the electron-impact excitation DCS for that line. The  $H(n=2)$  DCS from the CCC [4] was used for normalization of the continuum. The values  $T(E_1)$  are the analyzer transmission at  $E_1$  as determined by our He transmission runs. Error bars include Poisson statistical errors propagated by all subtractions (on the continuum and discrete features), uncertainty in the transmission of the analyzer, and uncertainties in the polynomial fitting to the continuum. We note that the uncer-

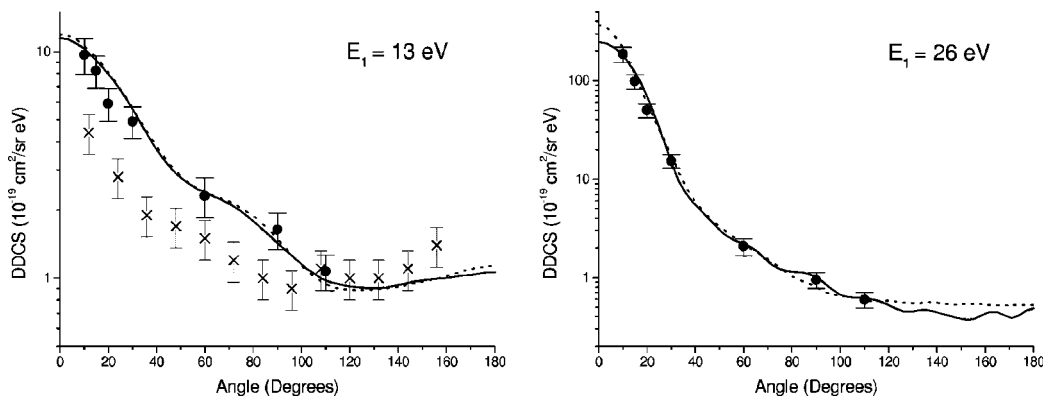


FIG. 5. Same as Fig. 4, but for  $E_0=40$  eV.

tainty in the transmission of the analyzer is the largest. We do not assume any errors in the DCS for the  $H(n=2)$  feature from the CCC calculation.

Figure 2 shows a selection of the DDCS taken at  $E_0=15.6$  eV and scattering angles from  $15^\circ$  to  $120^\circ$ . Agreement with theory is very good; however, we note that our DDCS are higher than theory by about 30–40% at small angles. Figure 3 shows a selection of the DDCS taken at  $E_0=17.6$  eV. Again, agreement with the CCC and the ECS models is very good; however, we note that the experimental DDCS's are about 30–40% lower on average in the near equal-energy-sharing conditions. We have critically investigated other sources of systematic errors (e.g., analyzer nose cone charging up due to the forward electron beam, background electrons from the needle and from gas-related sources) and could not find any other such corrections. In Fig 4, we present a selection of the DDCS taken at  $E_0=25$  eV where we also compare with the earlier measurements of Shyn [1]. Very good agreement is observed between our DDCS, the earlier measurements, and the ECS and CCC. Our DDCS are in especially good agreement with theory at  $E_1=11$  eV. Figure 5 shows a selection of the DDCS taken at  $E_0=40$  eV. Again, very good agreement is observed be-

tween our DDCS and the ECS and CCC, while the DDCS of Shyn are in poorer agreement with our DDCS and those of theory.

In summary, we have used a simple method (a movable  $H+H_2$  source) to determine accurate DDCS for the electron-impact ionization of H at energies close to threshold. Our experimental method is robust—we are able to obtain, after a relatively simple and direct data analysis, an energy-loss spectrum of background-free H. The measured DDCS instigated an improvement of the CCC calculation [15] which is now in good agreement with ECS. These measurements do not show complete agreement with theory, and it will be interesting to see how the minor discrepancies manifest themselves at other incident energies.

This project was funded by a grant from the National Science Foundation under Grant No. NSF-RUI-PHY-0096808. We acknowledge the expert help of technical staff Jorge Meyer (glass blowing shop), David Parsons (machine shop), and Hugo Fabris (electronics shop). M.B. acknowledges support from the U.S. Department of Energy, Office of Science.

- 
- [1] T.W. Shyn, *Phys. Rev. A* **45**, 2951 (1992).  
 [2] J. Röder, H. Ehrhardt, C. Pan, A.F. Starace, I. Bray, and D.V. Fursa, *Phys. Rev. Lett.* **79**, 1666 (1997).  
 [3] I. Bray and D.V. Fursa, *Phys. Rev. A* **54**, 2991 (1996).  
 [4] I. Bray, *J. Phys. B* **33**, 581 (2000).  
 [5] T.N. Rescigno, M. Baertschy, W.A. Isaacs, and C.W. McCurdy, *Science* **286**, 2474 (1999).  
 [6] M. Baertschy, T.N. Rescigno, W.A. Isaacs, X. Li, and C.W. McCurdy, *Phys. Rev. A* **63**, 022712 (2001).  
 [7] J. Röder, J. Rasch, K. Jung, C.T. Whelan, H. Ehrhardt, R.J. Allan, and H.R.J. Walters, *Phys. Rev. A* **53**, 225 (1996).  
 [8] I. Bray, *J. Phys. B* **32**, L119 (1999).  
 [9] M. Baertschy, T.N. Rescigno, and C.W. McCurdy, *Phys. Rev. A* **64**, 022709 (2001).  
 [10] I. Bray, *Aust. J. Phys.* **53**, 355 (2000).  
 [11] M.A. Khakoo, M. Larsen, B. Paolini, X. Guo, I. Bray, A. Stelbovics, I. Kanik, S. Trajmar, and G.K. James, *Phys. Rev. A* **61**, 012701 (1999).  
 [12] G.A. Keenan, I.C. Walker, and D.F. Dance, *J. Phys. B* **15**, 2509 (1982).  
 [13] B.P. Paolini and M.A. Khakoo, *Rev. Sci. Instrum.* **69**, 3132 (1998).  
 [14] G. Herzberg, *Spectra of Diatomic Molecules* (Van Nostrand, New York, 1950).  
 [15] I. Bray, *Phys. Rev. Lett.* **89**, 273201 (2002).  
 [16] D.V. Fursa and I. Bray, *Phys. Rev. A* **52**, 1279 (1995).  
 [17] A. Grafe, C.J. Sweeney, and T.W. Shyn, *Phys. Rev. A* **63**, 052715 (2001).